Fibers and Polymers 2015, Vol.16, No.3, 585-592
DOI 10.1007/s12221-015-0585-9

ISSN 1229-9197 (print version)
ISSN 1875-0052 (electronic version)

Electromagnetic Shielding Response of UV-induced Polypyrrole/Silver Coated Wool

Mazeyar Parvinzadeh Gashti*, Shima Tajzadeh Ghehi, Sara Valipour Arekhloo, Arash Mirsmaeeli, and Amir Kiumarsi[1]

Department of Textile, College of Engineering, Yadegar-e-Imam Khomeini (RAH) Branch, Islamic Azad University, Tehran 18155144, Iran

[1]*Chang School of Continuing Education, Ryerson University, Toronto M5B 2K3, Canada*

(Received August 1, 2014; Revised December 1, 2014; Accepted December 12, 2014)

Abstract: In this research, wool surface was successfully coated with polypyrrole (PPy) by one-step UV-induced polymerization using $AgNO_3$ as catalyst for oxidation of pyrrole monomers. The influence of the concentration of materials on the surface morphology, thermal and electromagnetic shielding properties was investigated using FTIR, XRD, SEM, EDS, TGA, RS and NA. The new bands at 2369 and 1519 cm^{-1} appeared in FTIR clearly showed structural changes of wool proteins. XRD spectra revealed two new peaks related to silver planes at $2\theta=33^{\circ}$ and 47° for UV-induced PPy/Ag nanocomposite coated wool. Furthermore, EDS results confirmed the presence of different amounts of silver on wool proportional to the applied PPy/Ag nanocomposites. TGA results demonstrated that the PPy/Ag nanocomposite coatings could significantly improve the thermal stability of wool fibers. This paper introduces a simple and versatile method for production of PPy/Ag nanocomposite, which can be applied as a high electromagnetic shielding on textiles.

Keywords: Wool, Thermal properties, Chemical analysis, Polypyrrole, Nano silver

Introduction

The procedures of inorganic/organic hybrid coatings of textiles have attracted a great deal of attention of researchers due to the synergistic surface and interface modifications of the substrate. Coatings are employed on textiles to induce desired characteristics such as antibacterial, super-hydrophobic, fire retardant, self-cleaning, super-hydrophilic, moth-proofing and electrical conductivity [1-5]. Various methods are utilized to embed nanoparticles (NPs) on the fiber surface including sol-gels technique, magnetron sputter coating, layer-by-layer (LBL) deposition method and polymer cross-linking [6].

The study of electromagnetic (EM) shielding properties of textiles coated with electrically conductive polymers is another field of interest to chemists [7-9]. Since EM wave is widely used in wireless communications and local networks, it may cause some interference problems in electronic devices, which in turn may reduce their lifetime. EM radiation may even cause harmful or injurious effects to humans and wildlife health if an EM field reaches a sufficient intensity [10]. To protect against EM radiation, textiles coated with metals such as Cu, Al, Ag, Au and Fe are used. The main disadvantages of metal-coated textiles are their low flexibility, limited wash fastness and poor abrasion resistant properties [11,12]. As alternative, conductive polymers such as polyaniline, polyacetylene, polythiophene and PPy are widely used as EM shielding materials for textile coatings [13]. Interestingly, EM shielding efficiency can be improved by combining metal NPs with conductive polymers for coating purposes [14]. Nanocomposites of PPy/Ag have been recently synthesized for eletrocatalysis, chemical and microelectronic sensors. In these approaches, silver nitrate is used as an oxidant for pyrrole and it will simultaneously be reduced to silver NPs. In the next step, PPy is polymerized very efficiently entrapping silver NPs within the polymer matrix and nanocomposite is formed. UV irradiation is used in this process to facilitate a rapid polymerization at ambient temperature [15-20]. Several research groups have produced organic/inorganic and inorganic/inorganic nanocomposites to investigate their electromagnetic interference shielding and microwave absorption. In this regard, nanocomposites of polyaniline/barium titanate [21], polyaniline/colloidal graphite [22], polyaniline/multi-walled carbon nanotube (MWCNT) [23], polyaniline/MWCNT/polystyrene [24], polyaniline/Fe_3O_4 [25], poly(3,4-ethylenedioxythiophene)/Fe_3O_4 [26], poly(methyl methacrylate)/graphene oxide [27], polystyrene/MWCNT/Graphite nanoplate [28,29], copolymers of aniline [30,31], nickel coated graphene [32], (Co^{2+}/Si^{4+}) substituted barium hexaferrites [33] with excellent electromagnetic interference shielding response and microwave absorption were studied.

Previous investigations on the pyrrole polymerization on wool had focused on the application of ferric chloride as the oxidant and anthraquinone-2-sulfonic acid as the dopant agents. The polymerizations were based on the aqueous and continuous vapor polymerization methods with further assessments of electrical and thermal conductivity of the wool [34-40].

In this respect, only two recent scientific reports have explained the chemical and UV induced polymerizations of PPy on cotton in the presence of silver ion as the oxidant. It was shown that silver plays an important role in the conductivity and antimicrobial activity of coated cotton

*Corresponding author: mparvinzadeh@gmail.com

samples [41,42].

However, to the best of our knowledge, there is no study on PPy/Ag nanocomposite coating of wool by UV irradiation. The proper investigation of EM reflection and transmission ratios of PPy/Ag network on wool is thus important to identify its potential EM shielding properties. The present work contributes to the studying of the morphological, physical and chemical properties of PPy/Ag nanocomposite coated wool fabric.

Experimental

Materials

Wool fabric was supplied by Moghadam Co., Iran. Nonionic detergent was provided by SDL Technologies for scouring the wool fabric. Pyrrole (C_4H_5N, >97 %) and silver nitrate ($AgNO_3$) were supplied by Merck Chemical Co., Germany.

Methods

Wool fabrics were scoured with 5 g/*l* nonionic detergent for 30 min at 50 °C. The L:G (liquor to good ratio) of the scouring solution was kept at 40:1. Fabric samples were then treated with solutions pyrrole and $AgNO_3$ (1:1) in deionized water at different concentrations (5, 15, and 25 % o.w.f) for 30 min under stirring. Photo-polymerizations of samples were accomplished under a UV lamp set at 254 nm (Germicidal UV lamp from Keosan Enterprise Co., South Korea, 15 W/ 0.3 A, light intensity: 0.4 μW/cm^2) for 30 min at ambient temperature [43]. The irradiated textiles were then washed separately with 1 g/*l* nonionic detergent at 40 °C for 15 min to remove any residual pyrrole, polypyrrole and silver nitrate. Finally, the fabrics were dried at 40 °C in an oven.

Characterization

The chemical compositions of the coated samples were evaluated using a FTIR spectroscopy [Bomem-MB 100 Series (Hartmann and Broun)].

A wide-angle X-ray diffractometry was utilized to study the crystalline changes of wool using a computerized SEIFERT/PTS 3003 X-ray diffractometer. Ni-filtered Cu-K_α radiation generated at 40 kV (k=0.1542 nm) and 30 mA was used. The measured angle ranged from 4 to 90 ° for untreated and nanocomposite coated fibers with a scan speed of 1 °/min.

The surface of fibers was also characterized using a Scanning Electron Microscope (SEM XL30, Philips). Samples were first coated with a thin layer of gold (w10 nm) by Physical Vapor Deposition method (PVD) using a sputter coater (SCDOOS, BAL-TEC). Silver was detected on all coated surfaces using the energy dispersive X-ray microanalysis (EDS) equipment attached to the SEM.

The thermogravimetric analysis (TGA) of the samples was performed on a TGA-PL thermo-analyzer from UK. In each case, a 5 mg sample was examined under N_2 at a heating elevation rate of 5 °C/min from room temperature to 600 °C.

The reflectance spectra of samples were recorded using a Gretagmacbeth COLOREYE 7000A Spectrophotometer integrated with an IBM personal computer.

The composite coated samples were finally evaluated for the electromagnetic reflection (*EMR*) and electromagnetic transmission (*EMT*) studies using the following equations according to ASTM D 4935-99:

$$EMR = |E_2 / E_1|^2 \quad (1)$$

$$EMT = |E_0 / E_1|^2 \quad (2)$$

where E_0, E_1 and E_2 are the electric field intensity transmitted through the fabrics, the electric field intensity of the field source and the electric field intensity reflected from the fabrics, respectively. The plane-wave was generated using a HP 8103C shielding effectiveness tester, which was connected to a network analyzer. The frequency was scanned from 5000 to 7800 MHz All parameters were measured in dB. The transmitter was set to an output level of 30 dBm.

Results and Discussion

Structural Information by FTIR Spectra

The infrared spectra of the untreated wool as well as a sample coated with 25 % PPy/Ag nanocomposite are shown in Figure 1. The peaks at 3435 and 1632 cm^{-1} are assigned to the N-H stretching of secondary amides and C=O stretching vibrations in wool proteins based on their chemical environment, the presence of intra- or intermolecular hydrogen bonds, and the types of amides. The bands at 2924, 870, 1227 and 1075 cm^{-1} can be assigned to C-H stretching, CH_2 out of plane bending, C-O-C asymmetric stretching and S-O-S (cysteine monoxide) vibrations, respectively [44,45].

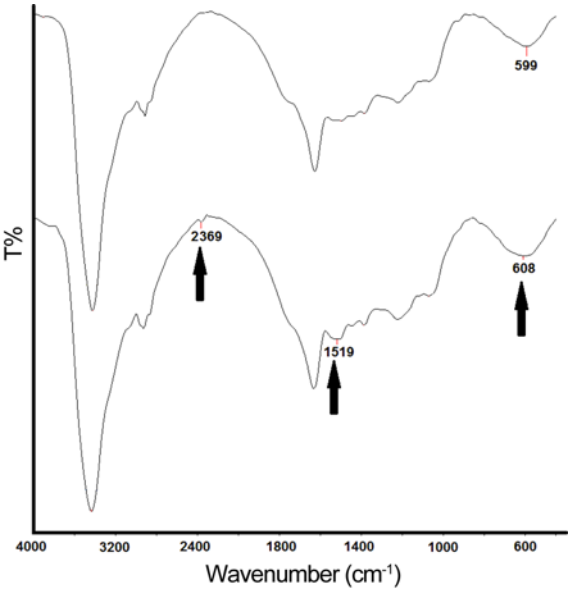

Figure 1. FTIR spectra of samples; (a) untreated wool and (b) wool coated with 25 % PPy/silver nanocomposite under UV irradiation.

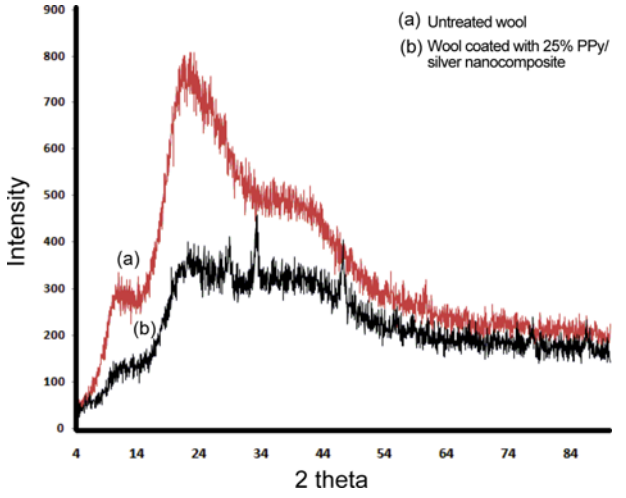

Figure 2. XRD patterns for untreated wool together with the sample coated with 25 % PPy/silver nanocomposite under UV irradiation.

Figure 1(b) shows the infrared spectra of wool fabric coated with 25 % PPy/Ag nanocomposite. There are two new bands appeared at 2369 and 1519 cm^{-1} which may be assigned to $C=N^{+}$ and N-H deformation of wool keratin structure. FTIR results clearly confirmed that the coating procedure of PPy/Ag on the wool surface was successful.

Evaluation of Coating by XRD

Figure 2 presents the X-ray diffractograms of the untreated wool and that of a UV cured sample coated with 25 % PPy/Ag nanocomposite. Wool fibers exhibit two typical diffraction peaks of hydrated crystals and α-keratin at $2\theta=11^{\circ}$ and 22° [46]. By comparing the diffractograms in Figure 2, it is evident that the intensities of these two peaks decreased in the coated wool with two new peaks appeared at $2\theta=33^{\circ}$ and 47° corresponding to (111) and (200) planes of silver, respectively [47]. The decline of the fiber diffraction intensity could be due to the presence of silver nanoparticles or a possible decrease in the crystalline fraction of fibers after coating process. It has been stated that the incorporation of nanoparticles in composites may result a different X-ray absorption pattern, which reduces the intensity of known values in resultant nanocomposites [48]. Previous studies have also showed that PPy has a broad diffraction peak in the range of $2\theta=20\text{-}35^{\circ}$ [49]. The superimposing of this peak with that of α-keratin along with the generation of two new peaks assigned to silver nanoparticles indicate the covering procedure of PPy/Ag nanocomposite on wool was successful.

Morphological Observation

Figure 3(a)-(e) presents the SEM images of untreated wool fiber and those of PPy/Ag nanocomposites coated (5 % and 25 %) and UV treated ones. The observed scales of untreated fiber showed no deposition of any type (Figure 3(a)) while the deposited silver nanoparticles with an average particle size of 24 nm was observed on the sample coated with 5 % PPy/Ag nanocomposite (Figure 3(b)). Moreover, the SEM images of 25 % PPy/Ag nanocomposite coated wool (Figures 3(d),(e)) showed a relatively homogenous coating on the fiber surface. Pyrrole was thus successfully polymerized under UV irradiation and silver nanoparticles were deposited both over the thin polymer layer or embedded within the matrix. A similar result was recently reported by Firoz Babu *et al.* by *in situ* chemical polymerization of PPy/Ag matrix on cotton fabric [41]. They stated that a redox reaction between silver ions and pyrrole monomers is responsible for the oxidation of polymer and reduction of silver ions to produce an inorganic/organic nanocomposite coating. The high magnification SEM image of the wool fibers coated with 25 % PPy/Ag nanocomposite (Figure 3(e)) also showed the formation of aggregated nanoparticles on the wool surface with an average particle size of 58 nm. It is evident that the increment of silver content in the coating increased the aggregation phenomenon of particles. This is clearly consistent with the authors previous studies on incorporating nanoparticles into the organic coatings [2,3,43].

The presence of silver on the fiber surface was investigated further by EDS analysis and the results are illustrated in Figure 3(f),(g). According to the patterns, gold (Au) was clearly sputtered on the untreated wool surface with no sign of the presence of silver (Ag). However, efficient interactions between the wool, silver ions and pyrrole monomer on the surface of wool fiber coated with of PPy/Ag nanocomposites lead to the presence of silver on the surface of samples. Unexpected lower values of silver content (1.87 and 5.48 wt.%) were observed for 5 % and 15 % PPy/Ag nanocomposite coated wool fibers, respectively. Similarly, Omastova *et al.* have recently detected 16.5 wt.% of silver on the surface of 73.6 % PPy/Ag composite film using EDS analysis [50]. This amount was extremely lower than the expected value expressing EDS to be a powerful tool for the surface characterization of the composites rather than the bulk ones [51,52].

Determination of Thermal Properties

Figure 4 shows the thermal degradation of the untreated wool and those of coated with 5 %, 15 % and 25 % PPy/Ag nanocomposites under UV light. The TGA curves of textiles generally consist of three sections of initial thermal degradation (1), main thermal degradation (2), and char decomposition stage (3). The change of the thermal properties and the weight loss of fibers are generally negligible in the first section. This can be due to the physical damages in the amorphous regions of the polymer chains or the removal of the surface adsorbed water molecules present on the fiber surface. Significant weight loss of all samples usually starts at about 230-250 $^{\circ}C$ as a result of thermal degradation of α-

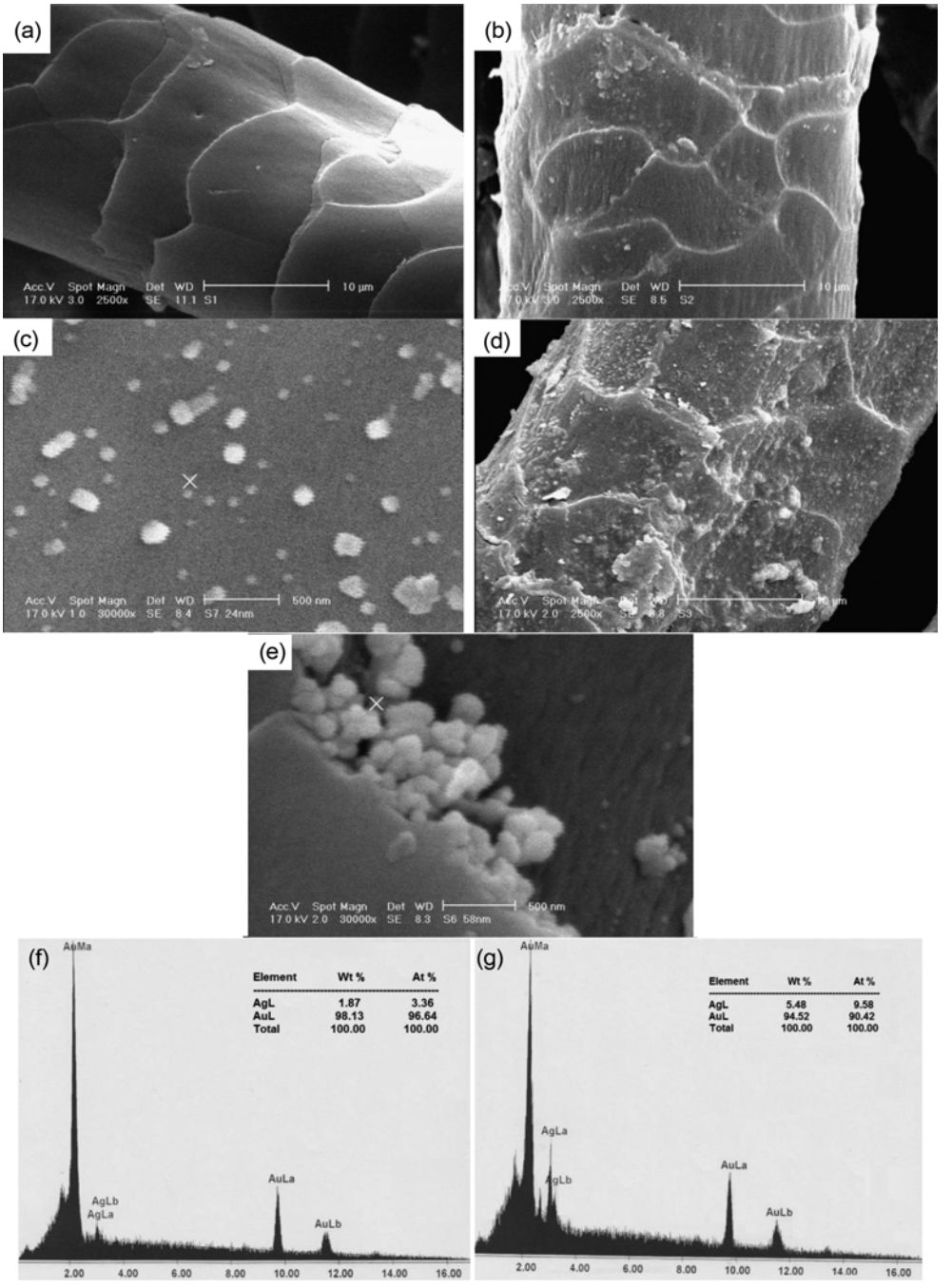

Figure 3. SEM images (a) untreated wool fiber at 2.5 KX, (b) wool fiber coated with 5 % PPy/silver nanocomposite under UV irradiation at 2.5 KX, (c) wool fiber coated with 5 % PPy/silver nanocomposite under UV irradiation at 30 KX, (d) wool fiber coated with 25 % PPy/silver nanocomposite under UV irradiation at 2.5 KX, (e) wool fiber coated with 25 % PPy/silver nanocomposite under UV irradiation at 30 KX, (f) EDX analysis of wool fiber coated with 5 % PPy/silver nanocomposite, and (g) EDX analysis of wool fiber coated with 25 % PPy/silver nanocomposite.

helices crystallites, keratin and other histological components of wool. Following the main thermal degradation of wool, water and carbon dioxide molecules as well as char residues are released at the third region at higher temperatures of 400 °C [53]. There was a considerable improvement in the thermal degradation curves (second region) of all nanocomposite coated samples in comparison with the untreated wool, confirming the heat insulating and barrier properties of the PPy/Ag nanoparticles coating layer [54]. The char contents of the coated samples were greater than the untreated wool,

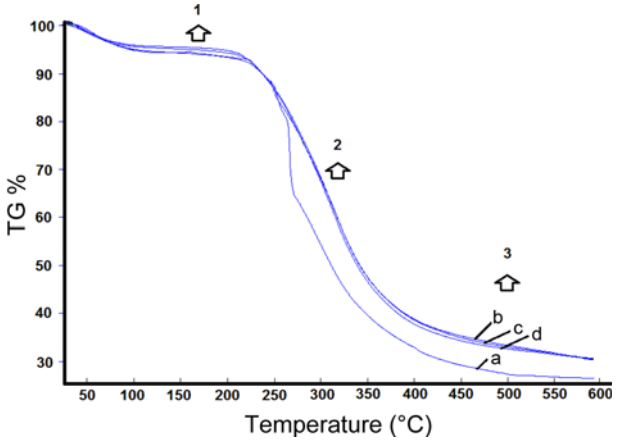

Figure 4. TGA curves of (a) untreated wool fiber, (b) wool fiber coated with 5 % PPy/silver nanocomposite under UV irradiation, (c) wool fiber coated with 5 % PPy/silver nanocomposite under UV irradiation, and (d) wool fiber coated with 25 % PPy/silver nanocomposite under UV irradiation.

stating the inclusion of inorganic/organic matrix on the fiber surface. The TGA results are in good agreement with EDS analysis.

Assessment of Optical and Colorimetric Properties

Figure 5 depicts the reflectance spectra of the untreated wool along with those of samples coated with different concentrations of PPy/Ag nanocomposites under UV irradiation. The reflectance of the untreated wool was higher than other samples, ranging between 45 % and 75 % in the considered spectral region. After coating wool with 5 % PPy/Ag nanocomposite, the reflection in the visible region decreased followed by further decline in reflectance values for the samples coated with 15 % and 25 % PPy/Ag nanocomposites. The major reflections of the coated substrates were mostly occurred at higher wavelengths (~600 nm) corresponding to the yellowish color. Such a color results from absorption a wide range of red and green wavelengths.

Variation of the L^*, a^* and b^* values for the untreated wool together with those of samples coated with different concentrations of PPy/Ag nanocomposites are given in Figure 6. CIELAB color space (L^*, a^* and b^*) is used for evaluating color coordinates. L^* is the color coordinate representing the lightness of sample. This parameter is assessed independently of color hue. Decrement in the lightness values among samples is a clear evidence of less reflectance. a^* is another measurable factor stating the horizontal red-green color axis while b^* is the variable value in vertical yellow-blue axis [53]. According to the results, the lightness (L^*) value decreased for the sample coated with 5 % PPy/Ag nanocomposite compared to the untreated wool and further decrease was observed as the concentration of PPy/Ag nanocomposite increased to 15 and 25 %. Increment in a^* and b^* values for wool coated with nanocomposites were also observed which could be due to

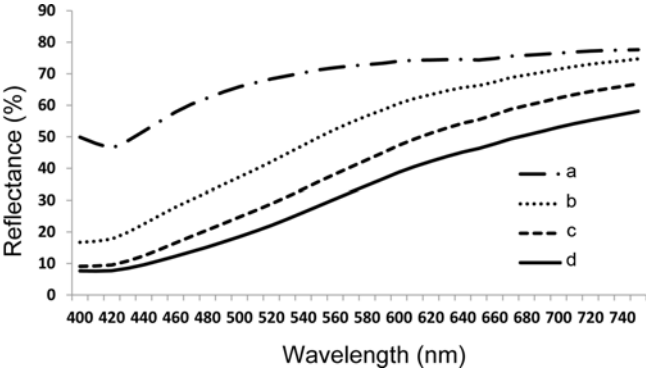

Figure 5. Reflectance curves of (a) untreated wool fiber, (b) wool fiber coated with 5 % PPy/silver nanocomposite under UV irradiation, (c) wool fiber coated with 5 % PPy/silver nanocomposite under UV irradiation, (d) wool fiber coated with 25 % PPy/silver nanocomposite under UV irradiation.

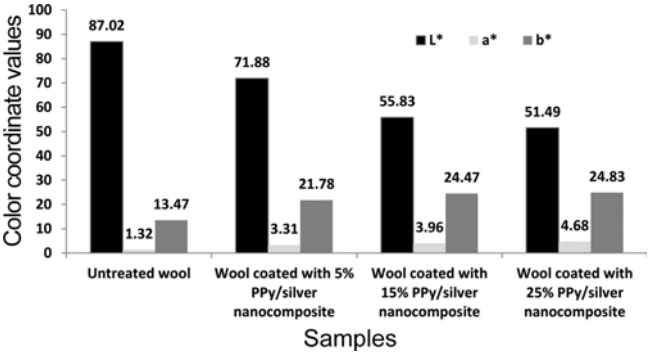

Figure 6. Color coordinates of the untreated wool fiber together with samples coated with different PPy/silver nanocomposites under UV irradiation.

optical properties of PPy layer and silver nanoparticles. The results for color changes of samples were in good agreement to those obtained from the reflectance measurements. The untreated wool had beige color, while the samples coated with 5, 15 and 25 % PPy/Ag nanocomposites displayed yellow to deep yellow and deep brown color, respectively. This could be due to the redox reaction between pyrrole monomer and silver ions [54].

Electromagnetic Properties of Nanocomposite Coated Samples

It is well known that the electrically charged devices are able to emit and receive EM waves. Reflection, absorption and/or internal reflection are the main source of attenuations, which occur when EM waves interact with different substrates, [55-60]. Basically, the EM transmission is described as the passage of the EM radiation through a textile (EMT). EM waves are also reflected from the textile boundaries (surface reflection) or their interior (volume reflection) known as the electromagnetic reflection (EMR). Moreover, radiation absorp-

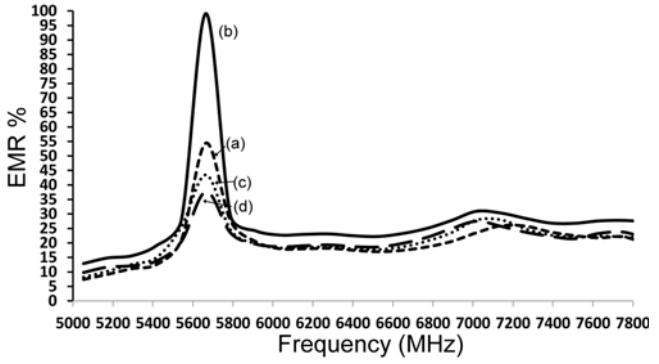

Figure 7. EMR% of untreated wool and those coated with different PPy/silver nanocomposites under UV irradiation. (a) wool coated with 15 % PPy/silver nanocomposite, (b) wool coated with 25 % PPy/silver nanocomposite, (c) wool coated with 5 % PPy/silver nanocomposite, and (d) untreated wool.

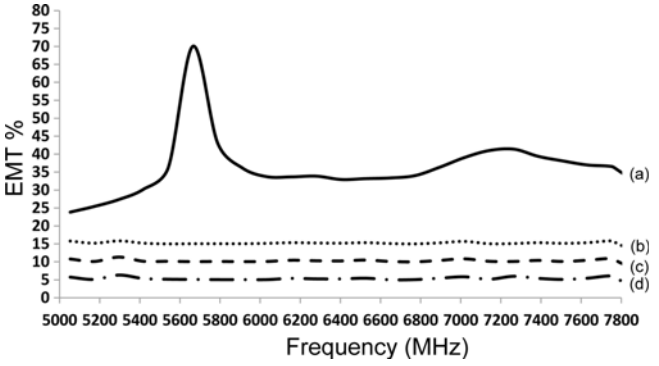

Figure 8. EMT% of untreated wool and those coated with different PPy/silver nanocomposites under UV irradiation; (a) untreated wool, (b) wool coated with 5 % PPy/silver nanocomposite, (c) wool coated with 15 % PPy/silver nanocomposite, and (d) wool coated with 25 % PPy/silver nanocomposite,

tion by textile substrates results in conversion of EM waves to another type of energy, usually heat [61-65].

Figures 7 and 8 illustrate EMR and EMT curves (5000-7800 MHz range) for the untreated wool and those of coated with different concentrations of PPy/Ag nanocomposites under UV irradiation. The reflection curve of untreated wool demonstrated a relatively intense peak at 5640 MHz, which was intensified in the nanocomposite coated samples. This peak reached a maximum of 95 % reflection for the sample coated with 25 % PPy/Ag nanocomposite. Although it was previously shown that conductive polymers have a great capability of absorbing and reflecting electromagnetic waves due to their intrinsic characteristics [66-69], it is now obvious that embedding silver nanoparticles within the PPy matrix improves the EM reflection of substrate. This advanced shielding property may be due to two main reasons as follows: Silver nanoparticles have a good conductivity and shallow skin depth, which enables them to act as EM shielding [70]; while PPy is also able to connect nanoparticle units thereby enhancing the reflection properties of nanocomposite coating [71]. Figure 8 clearly shows that the untreated wool encountered small fluctuation in transition from 33 to 42 % within the frequency range (5750-7800 kHz) while wool samples coated with 5 % PPy/Ag nanocomposite observed less EM transition. Any increase in PPy/Ag nanocomposite concentrations in coating caused an appropriate decrease in the EM transition. Larger amount of nanocomposite causing a strong polarization effect in conjugated structure of PPy might be the main reason of this behavior. It is noteworthy mentioning that the impedance of EM waves reflected from the untreated sample is not similar to those of coated substrates. Valence electrons of silver on the surface of coated wool can absorb EM waves causing them to change to excited state. This phenomenon is in good agreement with the results obtained in our previous studies [55-57].

Conclusion

In this study, PPy/Ag nanocomposites were successfully coated on wool using UV irradiation method. FTIR results confirmed the successful UV-polymerization of PPy based on the characteristic IR bands of the products. XRD of the products showed that the intensity of wool diffraction peaks is reduced due to the deposition of silver nanoparticles and PPy. Furthermore, SEM images of wool coated with PPy/Ag nanocomposites confirmed the formation of inorganic/organic matrix with an average particle size of 58 nm for silver. EDS results clearly confirmed that the silver content on the wool surface has been increased proportional to any increase in nanocomposite concentration. An improvement in the thermal degradation of nanocomposite coated wool samples to a certain extent was also observed which could be due to the high heat resistance, heat insulation effect, and mass transport barrier of silver particles embedded in PPy coating. The EMR and EMT properties of nanocomposite-coated samples were also influenced by conductive junctions of AgNPs within the PPy matrices. It is therefore concluded that silver incorporated PPy-coated wool is an effective lightweight EM shielding material for civil applications.

Acknowledgment

We thank Ghazaleh Chizari Fard and Shima Eslami for providing electromagnetic reflection and transmission images.

References

1. M. Niu, X. Liu, J. Dai, H. Jia, L. Wei, and B. Xu, *Fiber. Polym.*, **11**, 1201 (2010).
2. M. Parvinzadeh Gashti, F. Alimohammadi, and A. Shamei, *Surf. Coat. Technol.*, **206**, 3208 (2012).
3. F. Alimohammadi, M. Parvinzadeh Gashti, and A. Shamei,

Prog. Org. Coat., **74**, 470 (2012).
4. E. Pakdel and W. A. Daoud, *J. Colloid Interface Sci*., **410**, 1 (2013).
5. J. Bonastre, J. Molina, A. I. del Río, J. C. Galván, and F. Cases, *Synth. Met.*, **161**, 1958 (2011).
6. M. P. Gashti, *J. Text. Sci. Eng*. 4: e120. doi:10.4172/2165-8064.1000e120 (2014).
7. C. Y. Lee, D. E. Lee. C. K. Jeong, Y. K. Hong, J. H. Shim, J. Joo, M. S. Kim, J. Y. Lee, S. H. Jeong, S. W. Byun, D. S. Zang, and H. G. Yang, *Polym. Adv. Technol.,* **13**, 577 (2002).
8. A. Kaynak, E. Håkansson, and A. Amiet, *Synth. Met.,* **159**, 1373 (2009).
9. A. Oroumei, H. Tavanai, and M. Morshed, *J. Electron. Mater.,* **40**, 2256 (2011).
10. A. Zamanian and C. Hardiman, *High Frequency Electronics*, **4**, 16 (2005).
11. J. S. Roh, Y. S. Chi, T. J. Kang, and S. W. Nam, *Text. Res. J.,* **78**, 825 (2008).
12. J. Yip, S. Jiang, and C. Wong, *Surf. Coat. Technol.,* **204**, 380 (2009).
13. H. Deng, L. Lin, M. Ji, S. Zhang, M. Yang, and Q. Fu, *Prog. Polym. Sci.,* **39**, 627 (2014).
14. P. Saini, V. Choudhary, N. Vijayan, and R. K. Kotnala, *Phys. Chem. C*, **116**, 13403 (2012).
15. K. Jlassi, A. Singh, D. K. Aswal, R. Losno, M. Benna-Zayani, and M. M. Chehimi, *Colloid Surf. A-Physicochem. Eng. Asp.*, **439**, 193 (2013).
16. Y. Wei, L. Li, X. Yang, G. Pan, G. Yan, and X. Yu, *Nanoscale Res. Lett*., **5**, 433 (2010).
17. D. Hodko, M. Gamboa-Aldeco, and O. J. Murphy, *J. Solid State Electrochem.*, **13**, 1063 (2009).
18. X. Yang and Y. Lu, *Mater. Lett.*, **59**, 2484 (2005).
19. C. R. Martins, Y. M. de Almeida, G. C. do Nascimento, and W. M. de Azevedo, *J. Mater. Sci*., **41**, 7413 (2006).
20. A. Singh, Z. Salmi, N. Joshi, P. Jha, A. Kumar, H. Lecoq, S. Lau, M. M. Chehimi, D. K. Aswal, and S. K. Gupta, *RSC Adv.*, **3**, 5506 (2013).
21. P. Saini, M. Arora, G. Gupta, B. K. Gupta, V. N. Singh, V. Choudhary, and S. K. Dhawan, *Nanoscale*, **5**, 4330 (2013).
22. P. Saini, V. Choudhary, and S. K. Dhawan, *Polym. Adv. Technol.*, **20**, 355 (2009).
23. P. Saini, V. Choudhary, B. P. Singh, R. B. Mathur, and S. K. Dhawan, *Mat. Chem. Phys*., **113**, 919 (2009).
24. S. Maiti, N. K. Shrivastava, S. Suin, and B. B. Khatua, *ACS Appl. Mater. Interfaces*, **5**, 4712 (2013).
25. B. Zhang, Y. Du, P. Zhang, H. Zhao, L. Kang, X. Han, and P. Xu, *J. Appl. Polym. Sci.,* **130**, 1909 (2013).
26. W Zhou, X. Hu, X. Bai, S. Zhou, C. Sun, J. Yan, and P. Chen, *ACS Appl. Mater. Interfaces*, **3**, 3839 (2011).
27. S. N. Tripathi, P. Saini, D. Gupta, and V. Choudhary, *J. Mater. Sci.*, **48**, 6223 (2013).
28. P. Saini, V. Choudhary, B. P. Singh, R. B. Mathur, and S. K. Dhawan, *Synth. Met.*, **161**, 1522 (2011).
29. P. Saini, and M. Arora, Microwave Absorption and EMI Shielding Bahavior of Nanocomposites Based on Intrinsically Conducting Polymers, Graphene and Carbon Nanotubes, New Polymers for Special Applications, Dr. A. De Souza Gomes (Ed.), ISBN: 978-953-51-0744-6, InTech, DOI: 10.5772/48779. Available from: http://www.intechopen.com/books/new-polymers-for-special-applications/microwave-absorption-and-emi-shielding-behavior-of-nanocomposites-based-on-intrinsically-conducting-, 2012.
30. P. Saini and V. Choudhary, *J. Mater. Sci.,* **48**, 797 (2013).
31. P. Saini and M. Arora, *J. Mater. Chem. A,* **1**, 8926 (2013).
32. F. Jian-Jun, L. Su-Fang, Z. Wen-Ke, C. Hong-Yun, C. Jun-Fang, and C. Zong-Zhang, *J. Inorganic Mater.* **26**, 467 (2011).
33. S. M. Abbas, R. Chatterjee, A. K. Dixit, A. V. R. Kumar, and T. C. Goel, *J. Appl. Phys.,* **101**, 074105 (2007).
34. A. Varesano, L. Dall'Acqua, and C. Tonin, *Polym. Degrad. Stabil.*, **89**, 125 (2005).
35. L. Wang, T. Lin, X. Wang, and A. Kaynak, *Fiber. Polym.* **6**, 259 (2005).
36. A. Varesano, A. Aluigi, C. Tonin, and F. Ferrero, *Fiber. Polym.,* **7**, 105 (2006).
37. A. Boschi, C. Arosio, I. Cucchi, F. Bertini, M. Catellani, and G. Freddi, *Fiber. Polym*., **9**, 698 (2008).
38. A. Kaynak, S. Shaikhzadeh Najar, and R. C. Foitzik, *Synth. Met.,* **158**, 1 (2008).
39. A. Kaynak, L. Wang, C. Hurren, and X. Wang, *Fiber. Polym.,* **3**, 24 (2002).
40. S. Garg, C. Hurren, and A. Kaynak, *Synth. Met.,* **157**, 41 (2007).
41. K. Firoz Babu, P. Dhandapani, S. Maruthamuthu, and M. Anbu Kulandainathan, *Carbohydr. Polym.,* **90**, 1557 (2012).
42. M. F. Attia, T. Azib, Z. Salmi, A. Singh, P. Decorse, N. Battaglini, H. Lecoq, M. Omastova, A. A. Higazy, A. M. Elshafei, M. M. Hashem, and M. M. Chehimi, *J. Colloid Interface Sci.,* **393**, 130 (2013).
43. M. A. Breimer, G. Yevgeny, S. Sy, and O. A. Sadik, *Nano Lett.,* **6**, 305 (2011).
44. M. Parvinzadeh Gashti and A. Almasian, *Compos. Pt. B-Eng.,* **52**, 340 (2013).
45. M. Parvinzadeh Gashti, B. Katozian, M. Shaver, and A. Kiumarsi, *Color. Technol.,* **130**, 54 (2014).
46. J. Cao and C. A. Billows, *Polym. Int.*, **48**, 1027 (1999).
47. M. Parvinzadeh Gashti, and A. Almasian, *Compos. Pt. B-Eng.*, **43**, 3374 (2012).
48. R. Hajiraissi and M. Parvinzadeh, *Appl. Surf. Sci.,* **257**, 8443 (2011).
49. Y. Chen, Z. Zhao, and C. Zhang, *Synth. Met.,* **163**, 51 (2013).
50. M. Omastova, P. Bober, Z. Moravkova, N. Perinka, M. Kaplanova, T. Syrový, J. Hromadkova, M. Trchova, and J. Stejskal, *Electrochim. Acta*, **296**, 122 (2014).
51. M. Parvinzadeh, S. Moradian, A. Rashidi, and M. E. Yazdanshenas, *Appl. Surf. Sci.,* **256**, 2792 (2010).

52. M. Parvinzadeh, S. Moradian, A. Rashidi, and M. E. Yazdanshenas, *Polym.-Plast. Technol. Eng*., **49**, 1 (2010).
53. M. Melgosa, D. H. Alman, M. Grosman, L. Gómez-Robledo, A. Trémeau, G. Cui, P. A. García, D. Vázquez, C. Li, and M. Ronnier, *Color Res. Appl.,* **38**, 429 (2013).
54. S. Chatterjee, A. Garai, and A. K. Nandi, *Synth. Met.*, **161**, 62 (2011).
55. M. Parvinzadeh Gashti, A. Almasian, and M. Parvinzadeh Gashti, *Sens. Actuator A-Phys.,* **187**, 1 (2012).
56. M. Parvinzadeh Gashti and S. Eslami, *Superlattic. Microstruct*., **51**, 135 (2012).
57. M. Parvinzadeh and S. Eslami, *Res. Chem. Interm.*, **37**, 771 (2011).
58. D. D. L. Chung, *Carbon,* **39**, 279 (2001).
59. P. Saini, V. Choudhary, and S. K. Dhawan, *Polym. Adv. Technol.,* **23**, 343 (2012).
60. A. Kaynak and E. Hakansson, *Int. J. Cloth. Sci. Tech.*, **21**, 117 (2009).
61. P. Saini and V. Choudhary, *IJPAP,* **51**, 112 (2013).
62. P. Saini and V. Choudhary, *J. Appl. Polym. Sci.,* **129**, 2832 (2013).
63. A. Kaynak, E. Hakansson, and A. Amiet, *Synth. Met.,* **159**, 1373 (2009).
64. L. De C. Folgueras, E. L. Nohara, and M. C. Rezende, *Mat. Res.,* **10**, 95 (2007).
65. S. H. Kim, S. H. Jang, S. W. Byun, J. Y. Lee, J. S. Joo, S. H. Jeong, and M. J. Park, *J. Appl. Polym. Sci.,* **87**, 1969 (2003).
66. T. Mehmood, A. Kaynak, X. J. Dai, A. Kouzani, K. Magniez, D. Rubin de Celis, C. J. Hurren, and J. du Plessis, *Mater. Chem. Phys.,* **143**, 668 (2014).
67. Z. Yildiz, I. Usta, and A. Gungor, *Fibres Text. East. Eur.,* **21**, 32 (2013).
68. N. Onar, A. C. Aksit, M. F. Ebeoglugil, I. Birlik, and E. Celik, *J. Appl. Polym. Sci.,* **114**, 2003 (2009).
69. E. Håkansson, A. Amiet, and A. Kaynak, *Synth. Met.,* **156**, 917 (2006).
70. J. Ou, Y. Yang, Z. Yuan, Y. Zhang, L. Gan, and X. Chen, *Synth. Met.,* **195**, 9 (2014).
71. C. Y. Huang, J. Y. Wu, K. Y. Tsao, C. L. Lin, C. P. Chang, C. S. Tsai, Y. H. Chen, J. T. Yeh, and K. N. Chen, *Thin Solid Films*, **519**, 4765 (2011).